

SCALING IN-THE-WILD TRAINING FOR DIFFUSION-BASED ILLUMINATION HARMONIZATION AND EDITING BY IMPOSING CONSISTENT LIGHT TRANSPORT

Anonymous authors

Paper under double-blind review

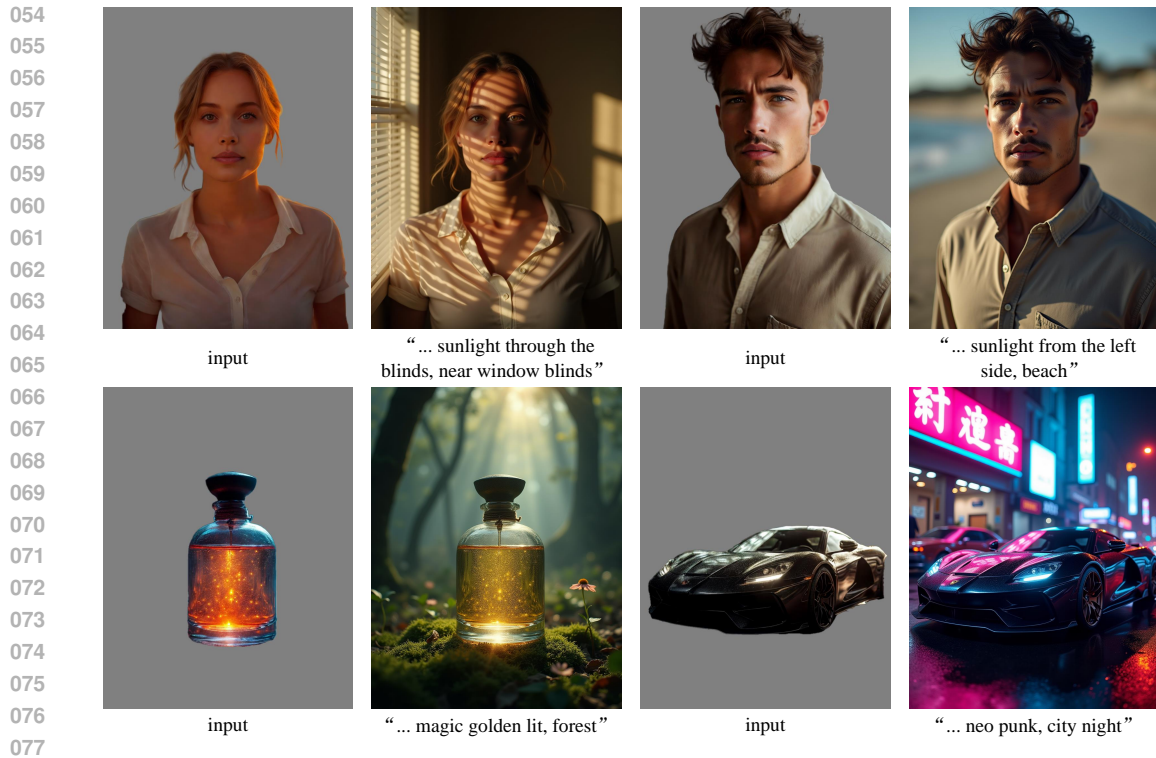
ABSTRACT

Diffusion-based image generators are becoming unique methods for illumination harmonization and editing. The current bottleneck in scaling up the training of diffusion-based illumination editing models is mainly in the difficulty of preserving the underlying image details and maintaining intrinsic properties, such as albedos, unchanged. Without appropriate constraints, directly training the latest large image models with complex, varied, or in-the-wild data is likely to produce a structure-guided random image generator, rather than achieving the intended goal of precise illumination manipulation. We propose Imposing Consistent Light (IC-Light) transport during training, rooted in the physical principle that the linear blending of an object’s appearances under different illumination conditions is consistent with its appearance under mixed illumination. This consistency allows for stable and scalable illumination learning, uniform handling of various data sources, and facilitates a physically grounded model behavior that modifies only the illumination of images while keeping other intrinsic properties unchanged. Based on this method, we can scale up the training of diffusion-based illumination editing models to large data quantities (>10 million), across all available data types (real light stages, rendered samples, in-the-wild synthetic augmentations, *etc.*), and using strong backbones (SDXL, Flux, *etc.*). We also demonstrate that this approach reduces uncertainties and mitigates artifacts such as mismatched materials or altered albedos.

1 INTRODUCTION

Editing the illumination in images is a fundamental task in deep learning and image editing. Classic computer graphics methods often model the appearance of images using physical illumination models. More recently, large diffusion-based image generators have introduced unique applications and flexible paradigms in this area, handling a wider range of “in-the-wild” lighting effects beyond simply changing the distribution of light sources, *e.g.*, generating backlighting or rim light, adding special effects like glow, glare, or the Tyndall effect, simulating shadows cast through tree shade or venetian blinds, and even manipulating human-drawn, composed, artistic, or non-photorealistic lighting conditions. These applications also provide tools for artists and designers to modify the foreground or background (*e.g.*, product images, commercial posters, *etc.*) while maintaining harmonious illumination. These illumination editing applications with generative image models hold unique industrial value for visual content creation and manipulation.

Diffusion-based illumination editing methods also present new opportunities and considerations for scaling up training and utilizing stronger backbones. Yet, training an illumination editing model at larger scales and with more diversity is more challenging than it seems. The first challenge lies in maintaining the desired model behavior to ensure proper illumination manipulation rather than deviating into unintended random behaviors. As the dataset size and diversity increase, the mapping and distribution of the learning objective can become ambiguous and uncertain. Without appropriate constraints, the training may produce a structure-guided random image generator, resulting in outputs that do not align with the desired illumination editing requirements. This deviation occurs when the model fails to learn a mapping corresponding to illumination modification, instead introducing



078
079
080
081
082

Figure 1: **Text-conditioned illumination modifying** with background generation (Flux.1-dev). We demonstrate the typical use case of this approach: users give an object image and illumination description, and our method generates corresponding object appearances and backgrounds.

083
084
085

arbitrary changes to the images, driven by dataset local minima or pretrained model default behaviors without proper alignments.

086
087
088
089
090
091
092
093
094
095

The second challenge is to preserve the underlying image details and intrinsic properties, such as albedo or reflectance colors, when modifying the illumination. Due to the stochastic nature of diffusion algorithms and the encoding-decoding processes of latent spaces, diffusion-based image generators inherently tend to introduce randomness into image contents, making it difficult to retain fine-grained details. Furthermore, effective illumination editing requires the model to have a thorough understanding of the scene to correctly adjust elements like shadows, highlights, and specular reflections. For instance, if the original image contains hard shadows, the model must first remove these existing shadows before adding new light sources and appropriate shadows. Preserving image details and intrinsic properties thus requires not only content generation but also discriminative and decomposition capabilities from the model to analyze image constituents. This necessitates careful design of training objectives and constraints to guide the learning process effectively.

096
097
098
099
100
101
102
103
104
105

In this paper, we propose a method to Impose Consistent Light (IC-Light) transport during training, grounded in the physical principle of light transport independence — the linear blending of an object’s appearances under different illumination conditions is consistent with its appearance under mixed illumination. By enforcing this consistency, we introduce a strong, physically-rooted constraint that ensures the model modifies only the illumination aspects of an image while preserving other intrinsic properties such as albedo and fine image details. This approach enables stable, scalable training on over 10 million diverse samples, including real photos from light stages, rendered images, and in-the-wild images with synthetic illumination augmentations. Our method demonstrates improved precision in illumination editing, reducing uncertainties and mitigating artifacts, without altering the underlying appearance details.

106
107

This method allows us to achieve a maximized setup: expanding the dataset to over 10 million images, adopting stronger backbones like SDXL and Flux, and utilizing all available types of data sources, including real photos captured from light stages, rendered images, and in-the-wild natural or artistic

108 images with synthetic illumination augmentations. We provide experimental evidence to validate that
109 increasing the training scale and diversifying data sources enhance model robustness and performance
110 in various illumination-related downstream tasks.

111 Ablation experiments demonstrate that applying the IC-Light method during training improves the
112 accuracy of illumination editing in preserving intrinsic properties like albedo and image details.
113 Furthermore, when compared to alternative models trained on smaller or more structured datasets, our
114 approach generalizes to a wider variety of illumination distributions, *e.g.*, rim lighting, backlighting,
115 magic glowing, sunset halo, *etc.* We also showcase the method’s ability to handle more in-the-wild
116 illumination scenarios, including artistic and composed lighting effects. Additionally, we explore
117 further applications, such as generating normal maps, and discuss the differences between this
118 approach and typical mainstream geometry estimation models.

119 In summary, (1) we propose IC-Light, a method for scaling up the training of diffusion-based
120 illumination editing models by imposing consistent light transport, ensuring precise illumination
121 modification while preserving intrinsic image details; (2) we provide pretrained illumination editing
122 models to facilitate illumination editing applications in content creation and manipulation across
123 diverse domains; (3) we present extensive experiments to validate the scalability and performance
124 of this approach, showing its difference from alternative methods in handling diverse illumination
125 conditions; (4) we present additional applications, such as normal map generation and artistic
126 lighting manipulation, further showcasing the versatility and robustness of our method in real-world,
127 in-the-wild scenarios.

128 129 2 RELATED WORK 130

131 **Image Illumination Editing with Deep Neural Networks** Learning-based methods have become
132 important baselines in image relighting over the past decade. Sun et al. (2019) utilized deep neural
133 networks to learn prior knowledge from light stage data. Nestmeyer et al. (2020) further enhanced the
134 neural network’s capability in relighting by modeling physical priors in the neural network training
135 process. Pandey et al. (2021) made use of high dynamic range (HDR) lighting maps (Debevec,
136 2008) to train relighting models by explicitly optimizing the Phong model prior. Various baselines
137 have been proposed to improve the efficiency, performance, and rationale of illumination modeling
138 (Zhou et al., 2019; Sengupta et al., 2021; Hou et al., 2021; 2022; Wang et al., 2023b; Zhou et al.,
139 2023). Switchlight (Kim et al., 2024) is a state-of-the-art relighting method trained with physically
140 co-designed neural networks for foreground relighting. 3D facial modeling (Shu et al., 2017) or
141 intrinsic images (Barron & Malik, 2014; Sengupta et al., 2018) have also been demonstrated to be
142 effective in portrait relighting. Illumination stylization can also facilitate portrait relighting (Shih
143 et al., 2014).

144 **Diffusion Models for Appearance and Illumination Manipulation** Recently, due to the develop-
145 ment of text-to-image diffusion models (Dhariwal & Nichol, 2021; Ho et al., 2020; Sohl-Dickstein
146 et al., 2015; Song et al., 2021), a wide range of tasks in image processing have seen significant
147 advancements (Ho & Salimans, 2021; Ho et al., 2022; Kawar et al., 2022a;b; Ramesh et al., 2022;
148 Rombach et al., 2022; Saharia et al., 2022; Zhang et al., 2023a; Wang et al., 2022). More specifically,
149 image editing (Alaluf et al., 2023; Brack et al., 2023; Brooks et al., 2023; Cao et al., 2023; Fu
150 et al., 2023; Han et al., 2024; Couairon et al., 2022; Hertz et al., 2022; Meng et al., 2021; Mokady
151 et al., 2022; Song et al., 2023; 2024; Tumanyan et al., 2023; Miyake et al., 2023; Zhang et al.,
152 2023b; Wu & De la Torre, 2023; Huberman-Spiegelglas et al., 2023; Wallace et al., 2022) and
153 paired image-to-image translation (Kwon & Ye, 2022; Nie et al., 2023; Sasaki et al., 2021; Wang
154 et al., 2022; Zhang et al., 2023a; Zhao et al., 2022) have shown that fine-tuning pretrained diffusion
155 models is an effective approach for manipulating the appearance of images. Text-to-image models
156 have also been proven effective in depth estimation (Ke et al., 2024), normal estimation (Fu et al.,
157 2024), and 3D construction (Anciukevičius et al., 2023; Chen et al., 2023a;b; Li et al., 2024; Lin
158 et al., 2023; Liu et al., 2023a; 2024b; 2023b; Tang et al., 2023; Metzger et al., 2022; Wang et al.,
159 2023c; Poole et al., 2022; Wang et al., 2023a; Xu et al., 2023). Relightful Harmonization (Ren et al.,
160 2024) is a state-of-the-art approach for manipulating the illumination of image foregrounds using
161 background conditions. More recently, DilightNet (Zeng et al., 2024), FlashTex (Deng et al., 2024),
and NeuralGaffer (Jin et al., 2024) have been proposed to manipulate object appearances mainly
based on 3D rendering data (and NeRF representations).

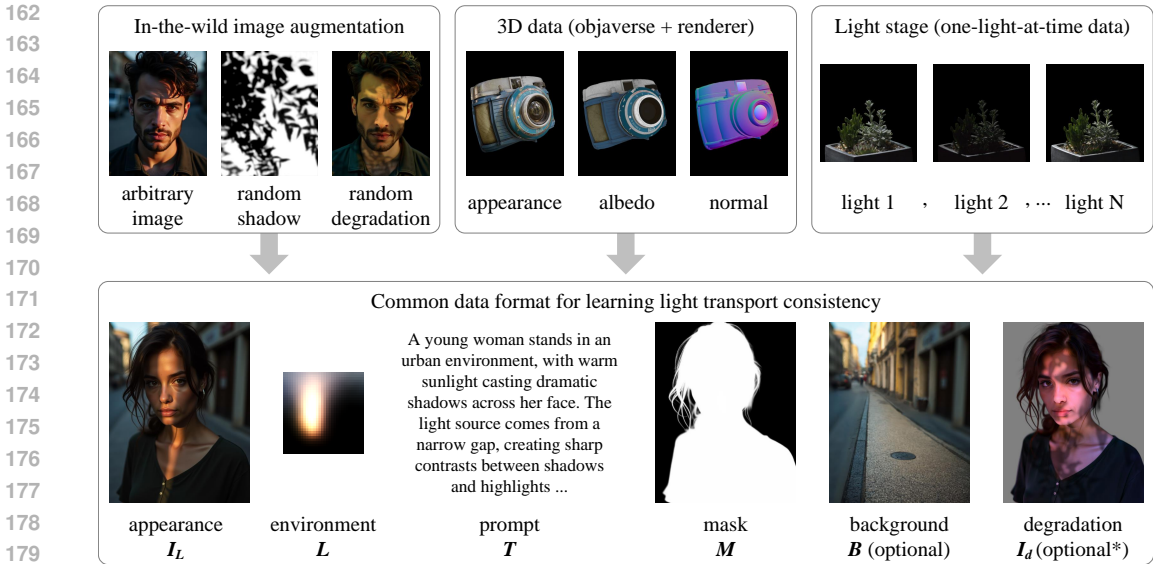


Figure 2: **Dataset collection.** We visualize various sources of the dataset and the components used during the training. Data from multiple sources are unified into a common format for neural network training. * Only “in-the-wild data augmentation” part has degradation images.

Light Stage Methods A light stage (Debevec et al., 2000) is a facility used to capture the appearance of real-world objects under different illumination conditions. Major recent progress has been made towards efficiency in light patterns and neural representations of different illuminations (Fyffe & Debevec, 2015; Ghosh et al., 2011; Meka et al., 2019). Human portrait processing has been considered an important direction in light stage research (Hou et al., 2021; 2022; Nestmeyer et al., 2020; Pandey et al., 2021; Sun et al., 2019; 2020; Yeh et al., 2022; Zhang et al., 2021; 2020). Wang et al. (2023b) pointed out that the sun can also be used as a special type of light stage. Calian et al. (2018) proposed modeling “light probes” for facial relighting. Sengupta et al. (2021) discussed that some real-world light sources can also be viewed as a light stage, like different images on desk monitor devices. Sevastopolsky et al. (2020) is another attempt to build an easier facility for more effective capturing of the light stage using a smartphone camera. Various illumination models (Debevec et al., 2000; Dorsey et al., 1995; Wenger et al., 2005) also depend on light stage measurements.

3 METHOD

We first discuss the illumination data distribution in Section 3.1, then detail the learning objective and training methods in Section 3.2.

3.1 IN-THE-WILD DATA DISTRIBUTION OF ILLUMINATION

As shown in Fig. 2, we model the distribution of illumination effects with multiple available types of data sources: arbitrary images, 3d data, and light stage images. These distributions allow capture of diverse and complex real-world lighting scenarios, *e.g.*, back light, rim light, glow, *etc.* For simplicity, we process all data to a common format. Every appearance image $I_L \in \mathbb{R}^{h \times w \times 3}$ is paired with a 32px environment map $L \in \mathbb{R}^{32 \times 32 \times 3}$, a foreground mask $M \in \mathbb{R}^{h \times w}$, an optional background image $B \in \mathbb{R}^{h \times w \times 3}$, and an optional degradation image $I_d \in \mathbb{R}^{h \times w \times 3}$.

In-the-wild image augmentation We use data augmentation to convert an arbitrary image into paired illumination training data. Specifically, we extract environment maps for an arbitrary image by randomly choosing between two methods: We either use the method of Phongthawee et al. (2023) or a custom environment-from-normal method detailed in the supplementary material. We detect foreground mask with Zheng et al. (2024) and generate background images with a distill-accelerated (Luo et al., 2023) Stable Diffusion inpainting model. We detect prompts using the method of Xiao

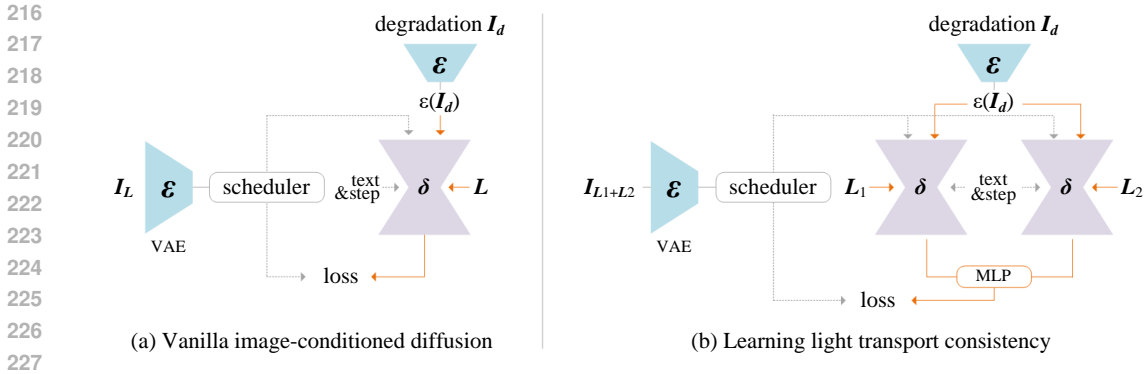


Figure 3: **Learning objective.** We visualize the learning objective of a vanilla image-conditioned diffusion model for illumination learning, and the learning objective for light transport consistency. The VAEs are frozen. Although this architecture is typical for UNet-based diffusion models, the same method also applies for (latent) diffusion transformers.

et al. (2023) or by using existing image prompts if the image is from text-image datasets. We then generate a “degradation appearance” that shares the same intrinsic albedo as the original image, but has completely altered illuminations; specifically we extract image albedo by randomly applying 6 albedo extraction methods in the supplementary materials. Then, we synthesize soft shadows using 3 random normal estimation methods, and synthesiz hard shadows with random shadow materials. Finally, we add a random level of specular reflection to random areas. See also the supplemental materials for full details. The shadow images are 20k high-quality shadow materials purchased from several online image stocks, and 500k generated materials using a Flux LoRA trained on those 20k purchased samples. Note that not all arbitrary images are suitable for illumination learning. We filtered 50M images to finalize 6M images by comparing the CLIP Vision similarity to key words “beautiful lighting”, “light”, and “illumination”.

3D rendering data We render Objaverse (Deitke et al., 2023) using a method similar to G-buffer Objaverse (Zuo et al., 2024). The difference is that we use an image-based rendering pipeline written in PyTorch for faster speed. We use random environment maps obtained from previous “in-the-wild image augmentation”, and use the method of Xiao et al. (2023) to detect prompts. We do not generate degradation images but directly use random unpaired environment map to render an altered appearance as I_d . The scale of this portion of our dataset is finalized at 4M images.

Light Stage We use multiple light stage datasets from Mnichelson (2006), Liu et al. (2024a), and an internal dataset with 20k light stage appearances. We pre-render all One-Light-At-a-Time (OLAT) data into the same aforementioned format. We use random environment maps obtained from previous “in-the-wild image augmentation”, use the method of Xiao et al. (2023) to detect prompts, and use random unpaired environment map to render altered appearances as I_d .

3.2 IMPOSING CONSISTENT LIGHT TRANSPORT

Our goal is to learn a robust and generalized model to handle in-the-wild illumination patterns. Nevertheless, learning the large-scale, complicated, and noisy data is challenging. Without well-suited regularization and constraints, the model can easily degrade to random behaviors that do not correspond to the intended illumination editing. Our solution is to Impose Consistent Light (IC-Light) transport during training, rooted in the physical principle that the linear blending of an object’s appearances under different illumination conditions is consistent with its appearance under a mixed illumination condition.

Vanilla objective We start with a vanilla image-conditioned diffusion model to learn the illumination without special constraints. As shown in Fig. 3-(a), taking a typical Stable Diffusion UNet as an example, we manipulate the UNet architecture to add 4 channels to the input convolution layer to receive I_d , the randomly relighted appearance of the target object or the degradation image. We

reshape any $32 \times 32 \times 3$ HDRI environment light source image \mathbf{L} to 3072 numbers and train a MLP from scratch with projection $3072 \rightarrow 4096 \rightarrow 4096 \rightarrow 4096 \rightarrow 2307$ (activated by Leaky RELU) and reshape the 2307 output numbers into a 3×768 embedding that can be directly received as a prompt embedding input with 3 tokens and 768 channels by SD 1.5. Given the target relighted image \mathbf{I}_L , latent diffusion algorithms first encode \mathbf{I}_L as a latent image $\epsilon(\mathbf{I}_L)$, and then progressively add noise to the latent image to produce a noisy latent $\epsilon(\mathbf{I}_L)_t$, where t represents the number of times noise is added. Given the set of conditions including time step t , illumination condition \mathbf{L} , as well as the input degradation \mathbf{I}_d , image diffusion algorithms learn the network δ to predict the noise with

$$\mathcal{L}_{\text{vanilla}} = \|\epsilon - \delta(\epsilon(\mathbf{I}_L)_t, t, \mathbf{L}, \mathcal{E}(\mathbf{I}_d))\|_2^2, \quad (1)$$

where ϵ is a diffusion target (noise or v-target for eps/v-prediction model, or flow target for flow match); $\mathcal{L}_{\text{vanilla}}$ is the cost function. Learning this objective allows for basic image relighting functionality with diffusion models. Besides, to train background-conditioned model, we concatenate \mathbf{B} to \mathbf{I}_d (and fill the extra channel with all zeros if some part of the dataset do not have backgrounds). Nevertheless, since the illumination data is challenging and noisy, this single objective will often lead to random model behaviors, *e.g.*, color mismatch, incorrect details, *etc.*

Light transport consistency In computational photography, light transport theory demonstrates that, considering arbitrary appearance \mathbf{I}_L^* and the correlated environment illumination \mathbf{L} , a matrix \mathbf{T} always exists so that

$$\mathbf{I}_L^* = \mathbf{T}\mathbf{L}, \quad (2)$$

where \mathbf{T} can be seen as $\mathbf{T} \in \mathbb{R}^{(h \times w \times 3) \times (32 \times 32 \times 3)}$ in our data format. The “*” indicates images in raw high-dynamic range. Real-world measurements (Debevec et al., 2000) validate that \mathbf{T} can always be represented with a single matrix, without any non-linear transforms. Because of this linearity, light transport explains appearance merging that

$$\mathbf{I}_{L_1+L_2}^* = \mathbf{T}(\mathbf{L}_1 + \mathbf{L}_2) = \mathbf{I}_{L_1}^* + \mathbf{I}_{L_2}^*, \quad (3)$$

where $\mathbf{L}_1, \mathbf{L}_2$ are two arbitrary environment illumination maps. This intuitively shows that the mixture of an object’s appearances under separate illuminations (*e.g.*, $\mathbf{L}_1, \mathbf{L}_2$) is equivalent to the appearance under merged illumination (*e.g.*, $\mathbf{I}_{L_1+L_2}^*$). This phenomenon is also validated by real-world measurements, *e.g.*, (Haeberli, 1992), and we attach related validating examples in the supplementary materials.

In this paper, we observe that the appearance \mathbf{I} in Eq. (3) can be replaced by arbitrary diffusion targets thanks to its linearity. For instance, consider a simple k-diffusion epsilon target at sigma-space step σ_t , estimated noise ϵ_L (conditioned on \mathbf{L}), and noisy image \mathbf{I}_{σ_t} , the estimated clean appearance can be written as $\hat{\mathbf{I}}_L = (\mathbf{I}_{\sigma_t} - \epsilon_L)/\sigma_t$. By applying Eq. (3) as $\hat{\mathbf{I}}_{L_1+L_2} = \hat{\mathbf{I}}_{L_1} + \hat{\mathbf{I}}_{L_2}$ we will also have $\epsilon_{L_1+L_2} = \epsilon_{L_1} + \epsilon_{L_2}$. As a result, the term in Eq. (3) can be replaced by any diffusion targets, *e.g.*, eps-prediction, v-prediction, flow match, *etc.*, as long as the target itself is linear and first-order.

The core idea of light transport consistency is to guarantee Eq. (3) during the diffusion training process so as to constrain the model to only modify image illumination without changing other intrinsic properties (*i.e.*, to keep the internal light transport \mathbf{T} unchanged). This can be achieved by minimizing $\|\mathbf{I}_{L_1+L_2}^* - (\mathbf{I}_{L_1}^* + \mathbf{I}_{L_2}^*)\|_2^2$ (where $\|\cdot\|_2$ is L2 norm). Using the aforementioned conversion, we can write it as a loss function for eps-prediction model $\|\epsilon_{L_1+L_2} - (\epsilon_{L_1} + \epsilon_{L_2})\|_2^2$.

For practical implementation, considering that most diffusion models are latent diffusion, we use a simple learnable Multi-Layer Perceptron (MLP) $\phi(\cdot, \cdot)$ to replace the sum term. Taking eps-prediction as an example, we have the final form of light transport consistency

$$\mathcal{L}_{\text{consistency}} = \|\mathbf{M} \odot (\epsilon_{L_1+L_2} - \phi(\epsilon_{L_1}, \epsilon_{L_2}))\|_2^2, \quad (4)$$

where $\phi(\cdot, \cdot)$ is a 5-layer MLP with hidden state 128, and input/output same as latent channels for different models, and \odot is pixel-wise multiplying with foreground mask \mathbf{M} (resized to same same as latent images). During training, we synthesize $\mathbf{L}_1, \mathbf{L}_2$ by generating random 4×4 masks from uniform distribution and resize the masks to same shape as \mathbf{L} , then, we view the masked area as \mathbf{L}_1 and unmasked areas as \mathbf{L}_2 , ensuring $\mathbf{L} = \mathbf{L}_1 + \mathbf{L}_2$. This loss function can be fully expanded as

$$\mathcal{L}_{\text{consistency}} = \|\mathbf{M} \odot (\epsilon - \phi(\delta(\epsilon(\mathbf{I}_{L_1})_t, t, \mathbf{L}_1, \mathcal{E}(\mathbf{I}_d))), \delta(\epsilon(\mathbf{I}_{L_2})_t, t, \mathbf{L}_2, \mathcal{E}(\mathbf{I}_d)))\|_2^2, \quad (5)$$

where each component is visualized in Fig 3-(b).

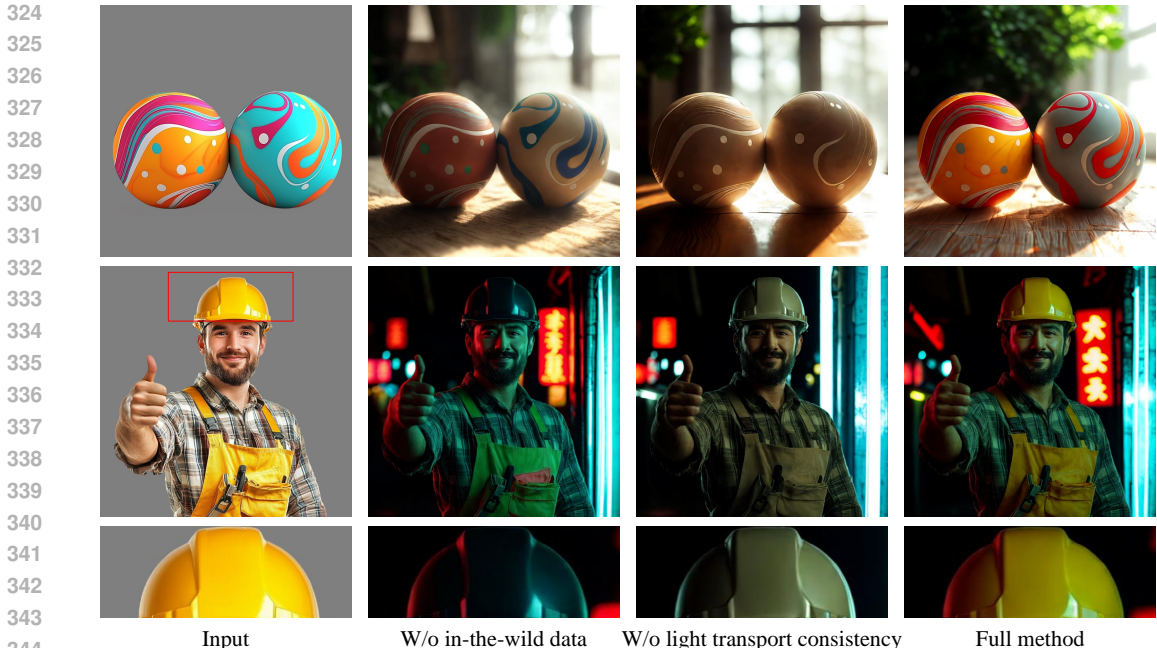


Figure 4: **Ablative Study.** We present results by removing the light transport consistency or in the wild data. More results are in the supplementary material. Results in this figure are from Stable Diffusion 1.5 version of our model.

Joint learning objective The final learning objective can be written as

$$\mathcal{L} = \lambda_{\text{vanilla}}\mathcal{L}_{\text{vanilla}} + \lambda_{\text{consistency}}\mathcal{L}_{\text{consistency}} , \tag{6}$$

where \mathcal{L} is the merged objective, and we use $\lambda_{\text{relight}} = 1.0, \lambda_{\text{consistency}} = 0.1$ as default weights.

4 EXPERIMENT

4.1 EXPERIMENTAL DETAILS

We use the AdamW optimizer with the learning rate of 1e-5 for training the entire framework. The pretrained Stable Diffusion models used are SD 1.5, SDXL, and Flux.1.0-dev. The training was conducted on 8 H100 80GB NVLink GPUs. We select the largest possible batch size for each model. For the SD 1.5 version of the model, the training took 100 hours. For the SDXL model, we first trained at 512 resolution for 80 hours, then fine-tuned at 1024 resolution for 60 hours.

The training process for the Flux model was more complex due to the large size of the Flux model. We adopted a multi-stage training strategy, where we separately trained the double-stream and single-stream parts of the model, using gradient freezing to freeze some parts of the gradient graph. This allowed us to train in larger batch sizes. More training details can be found in the supplementary material.

We use scheduled probability to balance the multiple training datasets, the in-the-wild image data and 3D rendering data appeared with equal probability during the initial stage of training. As training iterations increased, the probability of light stage data appearing in each batch increases. This allowed us to leverage a smaller portion of high-quality light stage data to improve the final model performance. In the beginning stages of training, the probabilities of in-the-wild data and 3D data were both 0.5, with light stage being 0.0. After 100,000 iterations, the probabilities were adjusted to 0.35 for in-the-wild data, 0.35 for 3D data, and 0.3 for light stage data. These probabilities were adjusted linearly throughout the training process.

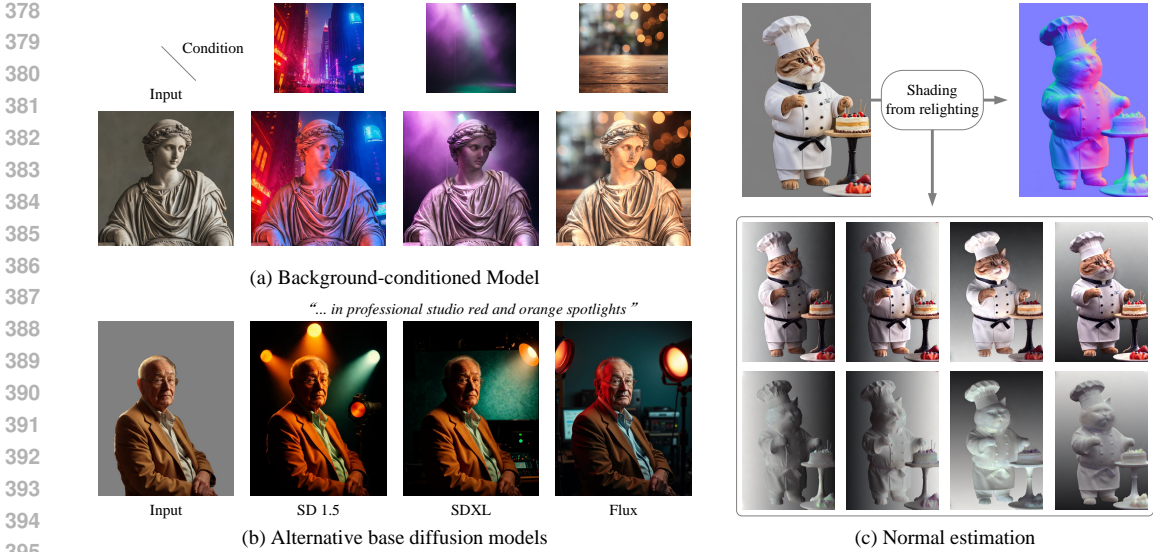


Figure 5: **Additional applications.** We show that this model supports more types of inputs like background conditions, and various base models like SD1.5/SDXL/Flux. We also show that multiple inferences of this method yields consistent appearances that can be merged into normal maps.

4.2 ABLATIVE STUDY

We conducted an ablative study to understand the importance of different components. We first remove the in-the-wild image augmentation data, meaning the model was trained only on 3D rendering data and light stage data. As seen in Fig. 4, removing in-the-wild data severely impacted the model’s generalization capability, especially for complex images like portraits. For example, hats on portraits that weren’t present in the training data would often be rendered in incorrect colors (e.g., changing from yellow to black).

We also experimented with removing the light transport consistency. Without this constraint, the model’s ability to generate consistent illumination and retain intrinsic properties such as albedo (reflectance color) significantly decreased. For example, the red and blue differences vanished in some images, and noticeable issues with color saturation are observed in the output.

The full method, which combines multiple data sources and enforces light transport consistency, produces a well-balanced model capable of generalizing across a range of scenarios. It also retains fine-grained image details and intrinsic properties, such as albedo, while reducing errors in output images. More examples are in the supplementary materials.

4.3 ADDITIONAL APPLICATIONS

As shown in the Fig. 5, we demonstrate additional applications such as using background conditions for illumination harmonization. Trained on extra channels for background conditions, our model can perform illumination generation conditioned solely on a background image without relying on environment maps. Additionally, our model supports different base models such as SD1.5, SDXL, and Flux, and the capabilities of these models are reflected in the generated results.

Multiple inferences from our method generate consistent appearances, which can be blended into normal maps. Specifically, for each object, we treat the global average of all relighted appearances as the albedo (diffuse color) A and divide the independent relighted appearances I_{L_i} by the albedo to obtain shadow maps S_{L_i} as

$$S_{L_i} = \frac{I_{L_i}}{A}, \tag{7}$$

where L_i is the i -th light source. The two vertical shadow maps $S_{L_{up}}$ and $S_{L_{down}}$ are averaged to form the green channel of the normal map N , and the two horizontal shadow maps $S_{L_{left}}$ and $S_{L_{right}}$ are

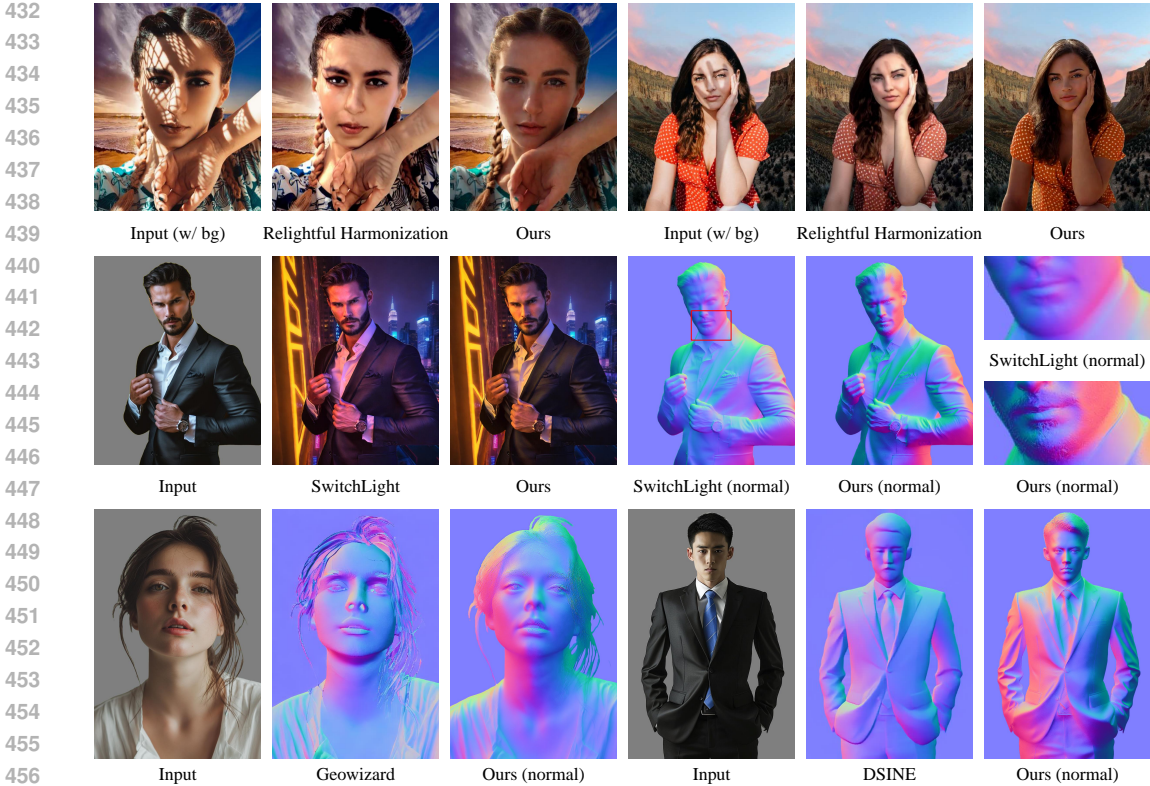


Figure 6: **Visual Comparison.** The Relightful Harmonization results are taken from official paper Ren et al. (2024) while other methods use official code bases or services.

averaged to form the red channel of the normal map as

$$N_{\text{green}} = \frac{S_{L_{\text{up}}} + S_{L_{\text{down}}}}{2}, \quad N_{\text{red}} = \frac{S_{L_{\text{left}}} + S_{L_{\text{right}}}}{2}. \quad (8)$$

Finally, the blue channel is padded to ensure the normal map N is a unit vector for each pixel as

$$N_{\text{blue}} = \sqrt{1 - N_{\text{red}}^2 - N_{\text{green}}^2}. \quad (9)$$

This process generates a complete normal map that can be used for further rendering tasks. We show examples in Fig. 5-(c).

4.4 VISUAL COMPARISON

We also conducted visual comparisons with previous methods. As seen in Fig. 6, compared to Relightful Harmonization (Ren et al., 2024), this model demonstrates higher robustness to shadows, thanks to a larger and more diverse training dataset. SwitchLight (Kim et al., 2024) and this model produces competitive relighting results. The quality of the normal maps of this method is a bit more detailed due to the methods of merging and deriving shadow from multiple appearances. Additionally, the normal maps produced by this model exhibit higher quality for human than alternatives GeoWizard (Fu et al., 2024) and DSINE (Bae & Davison, 2024).

4.5 QUANTITATIVE EVALUATION

We conducted quantitative comparisons using metrics such as Peak Signal-to-Noise Ratio (PSNR), Structural Similarity Index (SSIM), and Learned Perceptual Image Patch Similarity (LPIPS). We extracted a subset of 50,000 unseen 3D rendering data samples from the dataset for evaluation, ensuring that the model had not encountered these samples during training.

The tested methods are SwitchLight (Kim et al., 2024), DiLightNet (Zeng et al., 2024), and variants of our method without certain components (e.g., without light transport consistency, without augmentation data, without 3D data, and without light stage data). As shown in Table 1, our method outperforms others in terms of LPIPS, indicating superior perceptual quality. Models trained only on 3D data achieved the highest PSNR, but this is likely due to an evaluation bias towards the rendering data (since this test only uses 3D rendering data). The full method, which combines multiple data sources, achieved a balance between perceptual quality and performance across different metrics.

5 CONCLUSION

In this paper, we propose an approach for scaling up the training of diffusion-based illumination editing models by imposing consistent light transport (IC-Light). Our method ensures desired illumination manipulation while preserving intrinsic image properties, such as albedo and fine details. This is achieved through light transport consistency, a physically grounded constraint that helps stabilize training across diverse data sources, including in-the-wild images, 3D rendered data, and light stage captures. We demonstrate through extensive experiments and ablation studies that this approach reduces uncertainties, prevents artifacts, and improves model generalization to various illumination conditions. Additionally, our method supports a range of applications, such as background-aware relighting and normal map generation, and it scales to large datasets and strong model backbones like SDXL and Flux. The results validate a robust method well-suited for industrial and creative applications in image-based illumination editing.

REFERENCES

- Yuval Alaluf, Daniel Garibi, Or Patashnik, Hadar Averbuch-Elor, and Daniel Cohen-Or. Cross-image attention for zero-shot appearance transfer. *arXiv preprint arXiv:2311.03335*, 2023.
- Titas Anciukevičius, Zexiang Xu, Matthew Fisher, Paul Henderson, Hakan Bilen, Niloy J Mitra, and Paul Guerrero. Renderdiffusion: Image diffusion for 3d reconstruction, inpainting and generation. In *Proceedings of the IEEE/CVF Conference on Computer Vision and Pattern Recognition*, pp. 12608–12618, 2023.
- Gwangbin Bae and Andrew J. Davison. Rethinking inductive biases for surface normal estimation. In *IEEE/CVF Conference on Computer Vision and Pattern Recognition (CVPR)*, 2024.
- Jonathan T Barron and Jitendra Malik. Shape, illumination, and reflectance from shading. *IEEE transactions on pattern analysis and machine intelligence*, 37(8):1670–1687, 2014.
- Manuel Brack, Felix Friedrich, Dominik Hintersdorf, Lukas Struppek, Patrick Schramowski, and Kristian Kersting. Sega: Instructing diffusion using semantic dimensions. *arXiv preprint arXiv:2301.12247*, 2023.
- Tim Brooks, Aleksander Holynski, and Alexei A. Efros. Instructpix2pix: Learning to follow image editing instructions. In *Proceedings of the IEEE/CVF Conference on Computer Vision and Pattern Recognition (CVPR)*, pp. 18392–18402, June 2023.
- Dan A Calian, Jean-François Lalonde, Paulo Gotardo, Tomas Simon, Iain Matthews, and Kenny Mitchell. From faces to outdoor light probes. In *Computer Graphics Forum*, volume 37, pp. 51–61. Wiley Online Library, 2018.
- Mingdeng Cao, Xintao Wang, Zhongang Qi, Ying Shan, Xiaohu Qie, and Yinqiang Zheng. Masactrl: Tuning-free mutual self-attention control for consistent image synthesis and editing. *arXiv preprint arXiv:2304.08465*, 2023.

Table 1: Quantitative tests of ablative architectures and alternative methods.

Method	PSNR \uparrow	SSIM \uparrow	LPIPS \downarrow
SwitchLight	18.45	0.7024	0.3245
DiLightNet	21.78	0.8013	0.1721
w/o LTC	20.32	0.7542	0.1927
w/o aug. data	23.95	0.8723	0.1115
w/o 3d data	22.10	0.8041	0.1298
w/o light stage	23.70	0.8501	0.1077
Ours	23.72	0.8513	0.1025

- 540 Hansheng Chen, Jiatao Gu, Anpei Chen, Wei Tian, Zhuowen Tu, Lingjie Liu, and Hao Su. Single-
541 stage diffusion nerf: A unified approach to 3d generation and reconstruction. *arXiv preprint*
542 *arXiv:2304.06714*, 2023a.
- 543
544 Rui Chen, Yongwei Chen, Ningxin Jiao, and Kui Jia. Fantasia3d: Disentangling geometry and appear-
545 ance for high-quality text-to-3d content creation. In *Proceedings of the IEEE/CVF International*
546 *Conference on Computer Vision (ICCV)*, October 2023b.
- 547 Guillaume Couairon, Jakob Verbeek, Holger Schwenk, and Matthieu Cord. Diffedit: Diffusion-based
548 semantic image editing with mask guidance. *arXiv preprint arXiv:2210.11427*, 2022.
- 549
550 Paul Debevec. Rendering synthetic objects into real scenes: Bridging traditional and image-based
551 graphics with global illumination and high dynamic range photography. In *Acm siggraph 2008*
552 *classes*, pp. 1–10. 2008.
- 553 Paul Debevec, Tim Hawkins, Chris Tchou, Haarm-Pieter Duiker, Westley Sarokin, and Mark Sagar.
554 Acquiring the reflectance field of a human face. In *Proceedings of the 27th annual conference on*
555 *Computer graphics and interactive techniques*, pp. 145–156, 2000.
- 556
557 Matt Deitke, Dustin Schwenk, Jordi Salvador, Luca Weihs, Oscar Michel, Eli VanderBilt, Ludwig
558 Schmidt, Kiana Ehsani, Aniruddha Kembhavi, and Ali Farhadi. Objaverse: A universe of annotated
559 3d objects. In *CVPR*, pp. 13142–13153, 2023.
- 560 Kangle Deng, Timothy Omerick, Alexander Weiss, Deva Ramanan, Jun-Yan Zhu, Tinghui Zhou, and
561 Maneesh Agrawala. Flashtex: Fast relightable mesh texturing with lightcontrolnet. In *European*
562 *Conference on Computer Vision (ECCV)*, 2024.
- 563 Prafulla Dhariwal and Alexander Nichol. Diffusion models beat gans on image synthesis. *Advances*
564 *in Neural Information Processing Systems*, 34:8780–8794, 2021.
- 565
566 Julie Dorsey, James Arvo, and Donald Greenberg. Interactive design of complex time dependent
567 lighting. *IEEE Computer Graphics and Applications*, 15(2):26–36, 1995.
- 568
569 Tsu-Jui Fu, Wenzhe Hu, Xianzhi Du, William Yang Wang, Yinfei Yang, and Zhe Gan. Guid-
570 ing instruction-based image editing via multimodal large language models. *arXiv preprint*
571 *arXiv:2309.17102*, 2023.
- 572
573 Xiao Fu, Wei Yin, Mu Hu, Kaixuan Wang, Yuexin Ma, Ping Tan, Shaojie Shen, Dahua Lin, and
574 Xiaoxiao Long. Geowizard: Unleashing the diffusion priors for 3d geometry estimation from a
575 single image. *arxiv*, 2024.
- 576
577 Graham Fyffe and Paul Debevec. Single-shot reflectance measurement from polarized color gradient
578 illumination. In *2015 IEEE International Conference on Computational Photography (ICCP)*, pp.
579 1–10. IEEE, 2015.
- 580
581 Abhijeet Ghosh, Graham Fyffe, Borom Tunwattanapong, Jay Busch, Xueming Yu, and Paul Debevec.
582 Multiview face capture using polarized spherical gradient illumination. In *Proceedings of the 2011*
583 *SIGGRAPH Asia Conference*, pp. 1–10, 2011.
- 584
585 Paul Haeberli. Synthetic lighting for photography, 1992.
- 586
587 Ligong Han, Song Wen, Qi Chen, Zhixing Zhang, Kunpeng Song, Mengwei Ren, Ruijiang Gao,
588 Anastasis Stathopoulos, Xiaoxiao He, Yuxiao Chen, et al. Proxedit: Improving tuning-free real
589 image editing with proximal guidance. In *Proceedings of the IEEE/CVF Winter Conference on*
590 *Applications of Computer Vision*, pp. 4291–4301, 2024.
- 591
592 Amir Hertz, Ron Mokady, Jay Tenenbaum, Kfir Aberman, Yael Pritch, and Daniel Cohen-Or. Prompt-
593 to-prompt image editing with cross attention control. *arXiv preprint arXiv:2208.01626*, 2022.
- 594
595 Jonathan Ho and Tim Salimans. Classifier-free diffusion guidance. In *NeurIPS 2021 Workshop on*
596 *Deep Generative Models and Downstream Applications*, 2021.
- 597
598 Jonathan Ho, Ajay Jain, and Pieter Abbeel. Denoising diffusion probabilistic models. *Advances in*
599 *Neural Information Processing Systems*, 2020.

- 594 Jonathan Ho, Tim Salimans, Alexey Gritsenko, William Chan, Mohammad Norouzi, and David J
595 Fleet. Video diffusion models. 2022.
596
- 597 Andrew Hou, Ze Zhang, Michel Sarkis, Ning Bi, Yiyong Tong, and Xiaoming Liu. Towards high
598 fidelity face relighting with realistic shadows. In *Proceedings of the IEEE/CVF Conference on*
599 *Computer Vision and Pattern Recognition*, pp. 14719–14728, 2021.
- 600 Andrew Hou, Michel Sarkis, Ning Bi, Yiyong Tong, and Xiaoming Liu. Face relighting with
601 geometrically consistent shadows. In *Proceedings of the IEEE/CVF Conference on Computer*
602 *Vision and Pattern Recognition*, pp. 4217–4226, 2022.
603
- 604 Inbar Huberman-Spiegelglas, Vladimir Kulikov, and Tomer Michaeli. An edit friendly ddpm noise
605 space: Inversion and manipulations. *arXiv preprint arXiv:2304.06140*, 2023.
606
- 607 Haian Jin, Yuan Li, Fujun Luan, Yuanbo Xiangli, Sai Bi, Kai Zhang, Zexiang Xu, Jin Sun, and Noah
608 Snavely. Neural gaffer: Relighting any object via diffusion, 2024.
- 609 Bahjat Kawar, Roy Ganz, and Michael Elad. Enhancing diffusion-based image synthesis with robust
610 classifier guidance. *arXiv preprint arXiv:2208.08664*, 2022a.
611
- 612 Bahjat Kawar, Jiaming Song, Stefano Ermon, and Michael Elad. Jpeg artifact correction using
613 denoising diffusion restoration models. *arXiv preprint arXiv:2209.11888*, 2022b.
614
- 615 Bingxin Ke, Anton Obukhov, Shengyu Huang, Nando Metzger, Rodrigo Caye Daudt, and Konrad
616 Schindler. Repurposing diffusion-based image generators for monocular depth estimation. In
617 *Proceedings of the IEEE/CVF Conference on Computer Vision and Pattern Recognition (CVPR)*,
618 2024.
- 619 Hoon Kim, Minje Jang, Wonjun Yoon, Jisoo Lee, Donghyun Na, and Sanghyun Woo. Switchlight:
620 Co-design of physics-driven architecture and pre-training framework for human portrait relighting,
621 2024.
622
- 623 Gihyun Kwon and Jong Chul Ye. Diffusion-based image translation using disentangled style and
624 content representation. *arXiv preprint arXiv:2209.15264*, 2022.
- 625 Jiahao Li, Hao Tan, Kai Zhang, Zexiang Xu, Fujun Luan, Yinghao Xu, Yicong Hong, Kalyan
626 Sunkavalli, Greg Shakhnarovich, and Sai Bi. Instant3d: Fast text-to-3d with sparse-view generation
627 and large reconstruction model. In *International Conference on Learning Representations*, 2024.
628
- 629 Chen-Hsuan Lin, Jun Gao, Luming Tang, Towaki Takikawa, Xiaohui Zeng, Xun Huang, Karsten
630 Kreis, Sanja Fidler, Ming-Yu Liu, and Tsung-Yi Lin. Magic3d: High-resolution text-to-3d content
631 creation. In *IEEE Conference on Computer Vision and Pattern Recognition (CVPR)*, 2023.
632
- 633 Isabella Liu, Linghao Chen, Ziyang Fu, Liwen Wu, Haian Jin, Zhong Li, Chin Ming Ryan Wong,
634 Yi Xu, Ravi Ramamoorthi, Zexiang Xu, and Hao Su. Openillumination: A multi-illumination
635 dataset for inverse rendering evaluation on real objects, 2024a.
- 636 Minghua Liu, Ruoxi Shi, Linghao Chen, Zhuoyang Zhang, Chao Xu, Xinyue Wei, Hansheng Chen,
637 Chong Zeng, Jiayuan Gu, and Hao Su. One-2-3-45++: Fast single image to 3d objects with
638 consistent multi-view generation and 3d diffusion. *arXiv preprint arXiv:2311.07885*, 2023a.
639
- 640 Minghua Liu, Chao Xu, Haian Jin, Linghao Chen, Mukund Varma T, Zexiang Xu, and Hao Su.
641 One-2-3-45: Any single image to 3d mesh in 45 seconds without per-shape optimization. *Advances*
642 *in Neural Information Processing Systems*, 36, 2024b.
- 643 Yuan Liu, Cheng Lin, Zijiao Zeng, Xiaoxiao Long, Lingjie Liu, Taku Komura, and Wenping Wang.
644 Syncdreamer: Generating multiview-consistent images from a single-view image. *arXiv preprint*
645 *arXiv:2309.03453*, 2023b.
646
- 647 Simian Luo, Yiqin Tan, Suraj Patil, Daniel Gu, Patrick von Platen, Apolinário Passos, Longbo Huang,
Jian Li, and Hang Zhao. Lcm-lora: A universal stable-diffusion acceleration module, 2023.

- 648 Abhimitra Meka, Christian Haene, Rohit Pandey, Michael Zollhöfer, Sean Fanello, Graham Fyffe,
649 Adarsh Kowdle, Xueming Yu, Jay Busch, Jason Dourgarian, et al. Deep reflectance fields: high-
650 quality facial reflectance field inference from color gradient illumination. *ACM Transactions on*
651 *Graphics (TOG)*, 38(4):1–12, 2019.
- 652 Chenlin Meng, Yutong He, Yang Song, Jiaming Song, Jiajun Wu, Jun-Yan Zhu, and Stefano Ermon.
653 Sdedit: Guided image synthesis and editing with stochastic differential equations. In *International*
654 *Conference on Learning Representations*, 2021.
- 655 Gal Metzer, Elad Richardson, Or Patashnik, Raja Giryes, and Daniel Cohen-Or. Latent-nerf for
656 shape-guided generation of 3d shapes and textures. *arXiv preprint arXiv:2211.07600*, 2022.
- 657 Daiki Miyake, Akihiro Iohara, Yu Saito, and Toshiyuki Tanaka. Negative-prompt inversion: Fast
658 image inversion for editing with text-guided diffusion models. *arXiv preprint arXiv:2305.16807*,
659 2023.
- 660 Mnichelson. Light stage data gallery, vgl.ict.usc.edu/data/lightstage/, 2006.
- 661 Ron Mokady, Amir Hertz, Kfir Aberman, Yael Pritch, and Daniel Cohen-Or. Null-text inversion for
662 editing real images using guided diffusion models. *arXiv preprint arXiv:2211.09794*, 2022.
- 663 Thomas Nestmeyer, Jean-François Lalonde, Iain Matthews, and Andreas Lehrmann. Learning
664 physics-guided face relighting under directional light. In *IEEE Conf. Comput. Vis. Pattern Recog.*,
665 pp. 5124–5133, 2020.
- 666 Shen Nie, Hanzhong Allan Guo, Cheng Lu, Yuhao Zhou, Chenyu Zheng, and Chongxuan Li. The
667 blessing of randomness: Sde beats ode in general diffusion-based image editing. *arXiv preprint*
668 *arXiv:2311.01410*, 2023.
- 669 Rohit Pandey, Sergio Orts Escolano, Chloe Legendre, Christian Haene, Sofien Bouaziz, Christoph
670 Rhemann, Paul Debevec, and Sean Fanello. Total relighting: learning to relight portraits for
671 background replacement. *ACM Transactions on Graphics (TOG)*, 40(4):1–21, 2021.
- 672 Pakkapon Phongthawee, Worameth Chinchuthakun, Nontaphat Sinsunthithet, Amit Raj, Varun
673 Jampani, Pramook Khungurn, and Supasorn Suwajanakorn. Diffusionlight: Light probes for free
674 by painting a chrome ball. In *ArXiv*, 2023.
- 675 Ben Poole, Ajay Jain, Jonathan T Barron, and Ben Mildenhall. Dreamfusion: Text-to-3d using 2d
676 diffusion. *arXiv preprint arXiv:2209.14988*, 2022.
- 677 Aditya Ramesh, Prafulla Dhariwal, Alex Nichol, Casey Chu, and Mark Chen. Hierarchical text-
678 conditional image generation with clip latents. *arXiv preprint arXiv:2204.06125*, 2022.
- 679 Mengwei Ren, Wei Xiong, Jae Shin Yoon, Zhixin Shu, Jianming Zhang, HyunJoon Jung, Guido
680 Gerig, and He Zhang. Relightful harmonization: Lighting-aware portrait background replacement.
681 *CVPR*, 2024.
- 682 Robin Rombach, Andreas Blattmann, Dominik Lorenz, Patrick Esser, and Björn Ommer. High-
683 resolution image synthesis with latent diffusion models. In *Proceedings of the IEEE/CVF Confer-*
684 *ence on Computer Vision and Pattern Recognition (CVPR)*, pp. 10684–10695, June 2022.
- 685 Chitwan Saharia, William Chan, Huiwen Chang, Chris Lee, Jonathan Ho, Tim Salimans, David Fleet,
686 and Mohammad Norouzi. Palette: Image-to-image diffusion models. In *ACM SIGGRAPH 2022*
687 *Conference Proceedings*, pp. 1–10, 2022.
- 688 Hiroshi Sasaki, Chris G Willcocks, and Toby P Breckon. Unit-ddpm: Unpaired image translation
689 with denoising diffusion probabilistic models. *arXiv preprint arXiv:2104.05358*, 2021.
- 690 Soumyadip Sengupta, Angjoo Kanazawa, Carlos D Castillo, and David W Jacobs. Sfsnet: Learning
691 shape, reflectance and illuminance of faces in the wild. In *Proceedings of the IEEE conference on*
692 *computer vision and pattern recognition*, pp. 6296–6305, 2018.
- 693 Soumyadip Sengupta, Brian Curless, Ira Kemelmacher-Shlizerman, and Steven M Seitz. A light
694 stage on every desk. In *Proceedings of the IEEE/CVF International Conference on Computer*
695 *Vision*, pp. 2420–2429, 2021.

- 702 Artem Sevastopolsky, Savva Ignatiev, Gonzalo Ferrer, Evgeny Burnaev, and Victor Lempitsky.
703 Relightable 3d head portraits from a smartphone video. *arXiv preprint arXiv:2012.09963*, 2020.
704
- 705 YiChang Shih, Sylvain Paris, Connelly Barnes, William T Freeman, and Frédo Durand. Style transfer
706 for headshot portraits. *ACM Trans. Graph.*, 33(4):1–14, 2014.
- 707 Zhixin Shu, Sunil Hadap, Eli Shechtman, Kalyan Sunkavalli, Sylvain Paris, and Dimitris Samaras.
708 Portrait lighting transfer using a mass transport approach. *ACM Trans. Graph.*, 36(4):1, 2017.
709
- 710 Jascha Sohl-Dickstein, Eric Weiss, Niru Maheswaranathan, and Surya Ganguli. Deep unsupervised
711 learning using nonequilibrium thermodynamics. In *International Conference on Machine Learning*,
712 pp. 2256–2265. PMLR, 2015.
- 713 Jiaming Song, Chenlin Meng, and Stefano Ermon. Denoising diffusion implicit models. 2021.
714
- 715 Yizhi Song, Zhifei Zhang, Zhe Lin, Scott Cohen, Brian Price, Jianming Zhang, Soo Ye Kim, and
716 Daniel Aliaga. Objectstitch: Object compositing with diffusion model. In *Proceedings of the
717 IEEE/CVF Conference on Computer Vision and Pattern Recognition*, pp. 18310–18319, 2023.
- 718 Yizhi Song, Zhifei Zhang, Zhe Lin, Scott Cohen, Brian Price, Jianming Zhang, Soo Ye Kim,
719 He Zhang, Wei Xiong, and Daniel Aliaga. Imprint: Generative object compositing by learning
720 identity-preserving representation. *arXiv preprint arXiv:2403.10701*, 2024.
- 721 Tiancheng Sun, Jonathan T Barron, Yun-Ta Tsai, Zexiang Xu, Xueming Yu, Graham Fyffe, Christoph
722 Rhemann, Jay Busch, Paul Debevec, and Ravi Ramamoorthi. Single image portrait relighting.
723 *ACM Transactions on Graphics (TOG)*, 38(4):1–12, 2019.
- 724 Tiancheng Sun, Zexiang Xu, Xiuming Zhang, Sean Fanello, Christoph Rhemann, Paul Debevec,
725 Yun-Ta Tsai, Jonathan T Barron, and Ravi Ramamoorthi. Light stage super-resolution: Continuous
726 high-frequency relighting. *ACM Transactions on Graphics (TOG)*, 39(6):1–12, 2020.
727
- 728 Junshu Tang, Tengfei Wang, Bo Zhang, Ting Zhang, Ran Yi, Lizhuang Ma, and Dong Chen. Make-
729 it-3d: High-fidelity 3d creation from a single image with diffusion prior. In *Proceedings of the
730 IEEE/CVF International Conference on Computer Vision (ICCV)*, pp. 22819–22829, October 2023.
- 731 Narek Tumanyan, Michal Geyer, Shai Bagon, and Tali Dekel. Plug-and-play diffusion features for
732 text-driven image-to-image translation. In *Proceedings of the IEEE/CVF Conference on Computer
733 Vision and Pattern Recognition*, pp. 1921–1930, 2023.
- 734 Bram Wallace, Akash Gokul, and Nikhil Naik. Edict: Exact diffusion inversion via coupled transfor-
735 mations. *arXiv preprint arXiv:2211.12446*, 2022.
736
- 737 Tengfei Wang, Ting Zhang, Bo Zhang, Hao Ouyang, Dong Chen, Qifeng Chen, and Fang Wen.
738 Pretraining is all you need for image-to-image translation. 2022.
- 739 Tengfei Wang, Bo Zhang, Ting Zhang, Shuyang Gu, Jianmin Bao, Tadas Baltrusaitis, Jingjing Shen,
740 Dong Chen, Fang Wen, Qifeng Chen, et al. Rodin: A generative model for sculpting 3d digital
741 avatars using diffusion. In *Proceedings of the IEEE/CVF Conference on Computer Vision and
742 Pattern Recognition*, pp. 4563–4573, 2023a.
- 743 Yifan Wang, Aleksander Holynski, Xiuming Zhang, and Xuaner Zhang. Sunstage: Portrait recon-
744 struction and relighting using the sun as a light stage. In *Proceedings of the IEEE/CVF Conference
745 on Computer Vision and Pattern Recognition*, pp. 20792–20802, 2023b.
746
- 747 Zhengyi Wang, Cheng Lu, Yikai Wang, Fan Bao, Chongxuan Li, Hang Su, and Jun Zhu. Prolific-
748 dreamer: High-fidelity and diverse text-to-3d generation with variational score distillation. In
749 *Thirty-seventh Conference on Neural Information Processing Systems*, 2023c.
- 750 Andreas Wenger, Andrew Gardner, Chris Tchou, Jonas Unger, Tim Hawkins, and Paul Debevec.
751 Performance relighting and reflectance transformation with time-multiplexed illumination. *ACM
752 Trans. Graph.*, 24(3):756–764, 2005.
753
- 754 Chen Henry Wu and Fernando De la Torre. A latent space of stochastic diffusion models for zero-
755 shot image editing and guidance. In *Proceedings of the IEEE/CVF International Conference on
Computer Vision*, pp. 7378–7387, 2023.

- 756 Bin Xiao, Haiping Wu, Weijian Xu, Xiyang Dai, Houdong Hu, Yumao Lu, Michael Zeng, Ce Liu,
757 and Lu Yuan. Florence-2: Advancing a unified representation for a variety of vision tasks. *arXiv*
758 *preprint arXiv:2311.06242*, 2023.
- 759 Yinghao Xu, Hao Tan, Fujun Luan, Sai Bi, Peng Wang, Jiahao Li, Zifan Shi, Kalyan Sunkavalli,
760 Gordon Wetzstein, Zexiang Xu, and Kai Zhang. Dmv3d: Denoising multi-view diffusion using 3d
761 large reconstruction model, 2023.
- 762 Yu-Ying Yeh, Koki Nagano, Sameh Khamis, Jan Kautz, Ming-Yu Liu, and Ting-Chun Wang. Learning
763 to relight portrait images via a virtual light stage and synthetic-to-real adaptation. *ACM Trans.*
764 *Graph.*, 2022.
- 765 Chong Zeng, Yue Dong, Pieter Peers, Youkang Kong, Hongzhi Wu, and Xin Tong. Dilightnet:
766 Fine-grained lighting control for diffusion-based image generation. In *ACM SIGGRAPH 2024*
767 *Conference Papers*, 2024.
- 768 Longwen Zhang, Qixuan Zhang, Minye Wu, Jingyi Yu, and Lan Xu. Neural video portrait relighting
769 in real-time via consistency modeling. In *Proceedings of the IEEE/CVF International Conference*
770 *on Computer Vision*, pp. 802–812, 2021.
- 771 Lvmin Zhang, Anyi Rao, and Maneesh Agrawala. Adding conditional control to text-to-image
772 diffusion models. In *Proceedings of the IEEE/CVF International Conference on Computer Vision*,
773 pp. 3836–3847, 2023a.
- 774 Xuaner Zhang, Jonathan T Barron, Yun-Ta Tsai, Rohit Pandey, Xiuming Zhang, Ren Ng, and David E
775 Jacobs. Portrait shadow manipulation. *ACM Transactions on Graphics (TOG)*, 39(4):78–1, 2020.
- 776 Zhixing Zhang, Ligong Han, Arnab Ghosh, Dimitris N Metaxas, and Jian Ren. Sine: Single image
777 editing with text-to-image diffusion models. In *Proceedings of the IEEE/CVF Conference on*
778 *Computer Vision and Pattern Recognition*, pp. 6027–6037, 2023b.
- 779 Min Zhao, Fan Bao, Chongxuan Li, and Jun Zhu. Egsde: Unpaired image-to-image translation
780 via energy-guided stochastic differential equations. *Advances in Neural Information Processing*
781 *Systems*, 35:3609–3623, 2022.
- 782 Peng Zheng, Dehong Gao, Deng-Ping Fan, Li Liu, Jorma Laaksonen, Wanli Ouyang, and Nicu
783 Sebe. Bilateral reference for high-resolution dichotomous image segmentation. *CAAI Artificial*
784 *Intelligence Research*, 3:9150038, 2024.
- 785 Hao Zhou, Sunil Hadap, Kalyan Sunkavalli, and David W Jacobs. Deep single-image portrait
786 relighting. In *Proceedings of the IEEE/CVF International Conference on Computer Vision*, pp.
787 7194–7202, 2019.
- 788 Taotao Zhou, Kai He, Di Wu, Teng Xu, Qixuan Zhang, Kuixiang Shao, Wenzheng Chen, Lan Xu, and
789 Jingyi Yu. Relightable neural human assets from multi-view gradient illuminations. In *Proceedings*
790 *of the IEEE/CVF Conference on Computer Vision and Pattern Recognition*, pp. 4315–4327, 2023.
- 791 Qi Zuo, Xiaodong Gu, Yuan Dong, Zhengyi Zhao, Weihao Yuan, Lingteng Qiu, Liefeng Bo, and
792 Zilong Dong. High-fidelity 3d textured shapes generation by sparse encoding and adversarial
793 decoding. In *European Conference on Computer Vision*, 2024.
- 794
795
796
797
798
799
800
801
802
803
804
805
806
807
808
809